



Published in final edited form as:

Brain Behav Immun. 2019 February ; 76: 104–115. doi:10.1016/j.bbi.2018.11.010.

Removal of Microglial-Specific MyD88 Signaling Alters Dentate Gyrus Doublecortin and Enhances Opioid Addiction-like Behaviors

Phillip D. Rivera^{1,2,3,4,8}, Richa Hanamsagar^{1,2,3,8}, Matthew J. Kan^{5,6,7}, Phuong K Tran^{2,3}, David Stewart³, Young Chan Jo^{1,2}, Michael Gunn^{5,6}, and Staci D. Bilbo^{1,2,3,*}

¹Program in Neuroscience, Harvard Medical School, Boston, MA, USA.

²Department of Pediatrics, Lurie Center for Autism, MassGeneral Hospital for Children, Boston, MA, USA.

³Department of Psychology & Neuroscience, Duke University, Durham, NC, USA.

⁴Department of Biology, Hope College, Holland, MI, USA.

⁵Department of Immunology, Duke University Medical Center, Durham, NC, USA.

⁶Department of Medicine, Duke University Medical Center, Durham, NC, USA.

⁷Department of Pediatrics, University of California, San Francisco, CA, USA.

⁸Co-first authors

Abstract

Drugs of abuse promote a potent immune response in central nervous system (CNS) via the activation of microglia and astrocytes. However, the molecular mechanisms underlying microglial activation during addiction are not well known. We developed and functionally characterized a novel transgenic mouse (*Cx3cr1-CreBT^{tg/0}:MyD88^{f/f} [Cre^{tg/0}]*) wherein the immune signaling adaptor gene, *MyD88*, was specifically deleted in microglia. To test the downstream effects of loss of microglia-specific MyD88 signaling in morphine addiction, *Cre^{tg/0}* and *Cre^{0/0}* mice were tested for reward learning, extinction, and reinstatement using a conditioned place preference (CPP) paradigm. There were no differences in drug acquisition, but *Cre^{tg/0}* mice had prolonged extinction and enhanced reinstatement compared to *Cre^{0/0}* controls. Furthermore, morphine-treated *Cre^{tg/0}* mice showed increased doublecortin (DCX) signal relative to *Cre^{0/0}* control mice in the hippocampus, indicative of increased number of immature neurons. Additionally, there was an increase in colocalization of microglial lysosomal marker CD68 with DCX⁺ cells in morphine-treated *Cre^{tg/0}* mice but not in *Cre^{0/0}* or drug-naïve mice, suggesting a specific role for microglial MyD88 signaling in neuronal phagocytosis in the hippocampus. Our results show that *MyD88*

*Corresponding author: Staci Bilbo, 114 16th Street (Mail Stop 114-3400) Boston, MA 02129. sbilbo@mgh.harvard.edu.

Publisher's Disclaimer: This is a PDF file of an unedited manuscript that has been accepted for publication. As a service to our customers we are providing this early version of the manuscript. The manuscript will undergo copyediting, typesetting, and review of the resulting proof before it is published in its final citable form. Please note that during the production process errors may be discovered which could affect the content, and all legal disclaimers that apply to the journal pertain.

deletion in microglia may negatively impact maturing neurons within the adult hippocampus and thus reward memories, suggesting a novel protective role for microglia in opioid addiction.

Keywords

Microglia; extinction; morphine; neurogenesis; MyD88

Introduction

Drug abuse is a devastating mental illness, the study of which has largely focused on dopaminergic neurons from the ventral tegmental area (VTA) that connect to the nucleus accumbens (NAc) responsible for motivation and reward. More recently, microglia - the resident immune cell in the brain - have also been implicated in humans with substance use disorders (Onaivi et al. 2008; Sekine et al. 2008) as well as in multiple rodent studies (Ray et al. 2017; Metz et al. 2017; Bachtell et al. 2017; Schwarz, Hutchinson, and Bilbo 2011; Lacagnina et al. 2017). Direct interactions with drugs of abuse or their metabolites occur via toll-like receptors (TLRs) found on multiple cell types, with particular enrichment in microglia (Mark R. Hutchinson et al. 2010; Wang et al. 2012), which subsequently induce pro-inflammatory cytokine production (Mark R. Hutchinson et al. 2010; Stevens et al. 2013). There is growing evidence that the cytokines and chemokines produced downstream of TLR ligation by drugs of abuse impact the neural plasticity processes important in addiction. For example, murine whole-body knock-outs of *TLR4* and myeloid differentiation response protein 88 (*MyD88*), a critical co-adaptor protein of most TLRs, disrupt the acquisition of a rewarding memory using oxycodone conditioned place preference (CPP) (M. R. Hutchinson et al. 2012), a behavioral model used to examine drug/context associations (Bardo and Bevins 2000). While there is a growing appreciation for central immune signaling in addiction, it is unclear how microglia specifically mediate neuroimmune signaling in response to drugs of abuse, or how this signaling might alter learning and memory processes essential for reward memory.

CPP is a model of acute Pavlovian reinforcement following rewarding stimuli or non-rewarding stimuli. These stimuli require the hippocampus and its dentate gyrus (DG) sub-region to create drug/context associations. For example, lesions to the hippocampus lead to deficits in the formation of CPP reward memories (Ferbinteanu and McDonald 2001). This behavioral paradigm also appears to require adult hippocampal neurogenesis (hereafter referred to as AHNG) found within the DG. AHNG is the process of creating new neurons throughout life, whose functions include the integration of temporal and contextual information necessary to establish and maintain drug/context-associated reward learning and memory. For example, disruption of AHNG has been shown to influence extinction - new inhibitory learning over time - of reward memories after morphine (Bulin et al. 2017), cocaine self-administration (SA) (Noonan et al. 2010), and cocaine CPP (Castilla-Ortega et al. 2016). The process of AHNG is maintained by multiple mechanisms, including phagocytic activity by neural progenitors shaping AHNG (Lu et al. 2011), but notably also by apoptosis-driven phagocytosis by microglia (Sierra et al. 2014, 2010).

Microglial functions are well defined during central nervous system (CNS) development and include maintenance of neurogenesis, synapse formation, synapse elimination, and phagocytosis of apoptotic cells (Lacagnina, Rivera, and Bilbo 2017). Less is known about the functions of microglia under physiological conditions in adulthood. Microglia are likely important for synapse formation during learning and memory (Reshef et al. 2014; Parkhurst et al. 2013). For example, removal of *Cx3cr1* (fractalkine receptor, found primarily on microglia) leads to aberrant synaptic integration of adult-born neurons in the DG and deficits in anxiolytic-and depressive-like behaviors (Bolós et al. 2017), potentially through diminished AHNG (Bachstetter et al. 2011). Microglial phagocytosis is also impaired with the removal of *Cx3cr1* from the retina (Zabel et al. 2016) and brain (Bolós et al. 2017). Additionally, whole-body depletion of TLR4 signaling leads to enhanced memory retention for water maze and contextual fear memory (Okun et al. 2012). However, how microglia-specific TLR signaling may alter learning and memory, including reward learning, has yet to be defined.

Because microglia respond directly to morphine, they are well poised to sculpt AHNG via the phagocytosis of newborn neural precursor cells and therefore mediate drug/context associations and potentially other forms of learning and memory. Mouse studies have found that whole-body *TLR4* and *MyD88* knockout mice can differentially modulate AHNG (Rolls et al. 2007). We therefore examined if diminished microglia-specific *MyD88* signaling impacts AHNG and the response to a low dose of morphine, thereby affecting drug reward learning. We developed a novel transgenic mouse by crossing the *Cx3cr1-Cre* Bacterial Artificial Chromosome (BAC) transgenic (BT) mouse with *MyD88* floxed mice (i.e. *Cx3cr1-CreBT^{tg/0}.MyD88^{f/f}*). In doing so, pro-inflammatory signaling specifically in microglia is ablated within the CNS, without affecting *Cx3cr1* locus function. We hypothesized that, similar to whole-body knockouts of immune related signaling targets a depletion of neuro-immune signaling specifically from microglia would abolish the retrieval of a morphine/context association. Instead, we report a novel protective role for *MyD88* signaling in microglia in drug reward learning and maintenance, which has important implications for pan-cell inhibitors of inflammatory signaling in the treatment of addiction.

Materials & Methods

Animals

Cx3cr1-CreBT(MW126GSat) mice were generated and provided by L. Kus (GENSAT BAC Transgenic Project, Rockefeller University, New York, NY) and backcrossed over 12 generations on a C57BL/6N (Charles River) background. *MyD88-flox* (*MyD88*, Stock#: 008888, B6.129P2(SJL) -Myd88tm1Defr/J), *Rosa26-tdTomato* (Stock#: 007909, B6.Cg-Gt(ROSA) 26Sortm9(CAG-tdTomato)Hze/J), and *Rosa26-DTR* (Stock#: 007900, C57BL/6-Gt(ROSA) 26Sortm1(HBEGF)Awai/J) mice were purchased from Jackson Laboratories (Bar Harbor, ME). *MyD88*, *Rosa26-tdTomato*, and *Rosa26-DTR* mice were crossed with *Cx3cr1-CreBT* mice to produce *Cx3cr1-CreBT:MyD88*, *Cx3cr1-CreBT:Rosa26-tdTomato* (*Cx3cr1-CreBT:Rosa26-tdTomato*), and *Cx3cr1-CreBT:Rosa26-DTR* (*Cx3cr1-CreBT:DTR*) mice, respectively. Genotypes of the Cre and MyD88-flox transgene were identified via PCR using DNA from clipped tails. Primers for PCR genotyping: MyD88, Fwd - GTT GTG TGT GTC

CGA CCG T, Rev - GTC AGA AAC AAC CAC CAC CAT GC: Cre, Fwd - TTC GGC TAT ACG TAA CAG GG, Rev - TCG ATG CAA CGA GTG ATG AG: tdTomato^{Mut/Mut}, Fwd - CTG TTC CTG TAC GGC ATG G, Rev - GGC ATT AAA GCA GCG TAT CC: tdTomato^{WT/WT}, Fwd - AAG GGA GCT GCA GTG GAG TA, Rev -CCG AAA ATC TGT GGG AAG TC. *Cx3cr1-CreBT^{tg/0}:MyD88^{ff/f}* mice (Cre^{tg/0}) functioned as the experimental group (*MyD88* impairment in microglia) while *Cx3cr1-CreBT^{0/0}:MyD88^{ff/f}* (Cre^{0/0}) mice functioned as the control group (*MyD88* intact in microglia). To assess transgenic differences, C57BL/6N wild-type (Charles River Laboratories, Raleigh, NC) animals were used as wild-type (WT) controls. All mice used were between 8 and 12 weeks old. Diphtheria toxin (DT) (List Biological Laboratories, Inc., Campbell, CA) was resuspended in 1X PBS and mice were injected i.p. with 150 ng/g DT in 100 μ L of PBS every 24 hours (hrs) for 3 days. Body weight of DT-treated mice was monitored daily. All animal experiments were conducted in accordance with National Institutes of Health guidelines and protocols approved by the Animal Care and Use Committee at Duke University.

Tissue collection

Mice were deeply anesthetized with a ketamine/xylazine cocktail (430 mg/kg ketamine; 65 mg/kg xylazine i.p.) and transcardially perfused with ice-cold 0.9% saline for 2 minutes (min) to clear brains of blood. Brains were rapidly extracted and homogenized for microglia isolations or placed into 4% PFA and cryoprotected with 30% sucrose in 0.1% sodium azide for histological experiments. All tissue collection occurred in the light cycle between 10 AM and 2 PM.

Primary cell isolations

Whole brain without cerebellums were isolated post-perfusion from adult WT, Cre^{0/0}, and Cre^{tg/0} animals and were homogenized in enzyme digestion mix containing collagenase A (1.5 mg/mL, Roche, Indianapolis, IN, USA) and DNase I (0.4 mg/mL, Roche, Indianapolis, IN, USA) in Hank's Buffered Salt Solution (HBSS, Thermo Fisher Scientific, Waltham, MA) for 45 min in a 37°C water bath. Every 15 min during the incubation, samples were removed from the water bath and passed through glass Pasteur pipettes multiple times to ensure complete dissociation. Samples were then filtered through nylon filter and centrifuged at 1200 rpm for 10 min at 4°C. For microglial isolation experiments, cell pellets were resuspended in 5 mL of 30% Percoll in 1X PBS (GE Healthcare, Uppsala, Sweden) prepared from isotonic percoll (ITP, containing 90% Percoll and 10% 10X PBS, Thermo Fisher Scientific, Waltham, MA) and underlaid carefully with 4 mL 70% Percoll in 1X PBS prepared from ITP. Samples were centrifuged at 1400 rpm for 15 min at 23°C with no brake. The interphase containing mostly mononuclear phagocytes was isolated and counted. Cells were incubated with CD11b antibody-conjugated magnetic beads (MACS Miltenyi Biotec, San Diego CA) for 15 min at 4°C, in a concentration based on manufacturer's recommendations. After washing, cells were passed through a magnetic bead column (MACS Miltenyi Biotec, San Diego CA) and CD11b positive (CD11b⁺) and negative (CD11b⁻) populations were separated. Isolated cells were centrifuged at 1200 rpm, 10 min, 4°C, following which supernatant was aspirated and cell pellets were resuspended in 200 μ L of medium (2 mM L-glutamine, 1% penicillin-streptomycin, 1X N2 supplement media, 1 mM sodium pyruvate, 50 μ g/mL Forskolin in 1X DMEM). All cells were counted using

hematocytometer and total number of cells were determined for each sample. A minimum of 30,000 microglial cells were plated per well for U-bottom, 96-well plate. 100 uL of cell suspension and 100 uL of treatment (made in same microglia medium) was added to each well. Cells were treated in triplicate: Media only or lipopolysaccharide (LPS, 10 ng/mL, from *Escherichia coli* 055:B5, L6529, Sigma-Aldrich, St. Louis, MO). Cells were incubated at 37°C for 2 or 4 hrs in 5% CO₂, 95% O₂. After the treatment was complete, plates were centrifuged, supernatant was separated out and frozen at –80°C for future protein analysis. Trizol was added to cell pellets and frozen at –80°C until ready for RNA extraction.

For co-culture experiments, Cre^{0/0} and Cre^{tg/0} mice (n=2 genotype/treatment) were administered morphine (3 mg/kg morphine) or saline 1 hr prior to sacrifice. All steps were performed similar to the microglial isolations described above, except where noted below. Samples were pooled per genotype/treatment during nylon filtration and no percoll step was performed. For immature neuron isolations, cells were incubated with PSA-NCAM antibody-conjugated magnetic beads (MACS Miltenyi Biotec, San Diego CA) for 15 min at 4°C, in a concentration based on manufacturer's recommendations. After washing, cells were passed through a magnetic bead column (MACS Miltenyi Biotec, San Diego CA) and PSA-NCAM positive (PSA-NCAM⁺) and negative (PSA-NCAM⁻) populations were separated. Microglial isolations were performed as described above on the PSA-NCAM⁻ population. A minimum of 20,000 microglia and 100,000 immature neurons were plated per well on a round cover glass within a 24-well plate. Cells were plated in triplicate for each genotype/treatment group. A total of 500uL of PSA-NCAM cells in medium (described above) were incubated at 37°C for 1 hr in 5% CO₂, 95% O₂. 100 uL of CD11b⁺ cells were then overlaid on PSA-NCAM⁺ neurons and were incubated (as above) for 1 hr. Cells were fixed with 4% PFA for 10 min, rinsed with 1X PBS, and stored at 4°C.

RNA extraction, quantification and purity determination

Frozen samples or isolated cells were homogenized in 800 uL TRIzol® (Thermo Fisher Scientific, Waltham, MA) followed by vortexing at 2000 rpm for 10 min. 160 uL of chloroform (Thermo Fisher Scientific, Waltham, MA) was added to each tube and vortexed for additional 2 min. Samples were then centrifuged at 11,800 rpm for 15 min at 4°C, after which the top clear aqueous phase was separated into a fresh tube. Following this, 2 uL of Glycogen (Thermo Fisher Scientific, Waltham, MA) was added to the aqueous phase followed by 360 mL of Isopropanol (Thermo Fisher Scientific, Waltham, MA). Samples were vortexed for 1 min and centrifuged. Supernatant was discarded carefully without disturbing RNA pellet. Pellets were washed two times with 1 mL of ice cold 75% ethanol, air dried and resuspended in 6–8 uL of RNase-free water. Preliminary RNA quantification and purity determination was done using NanoDrop Spectrophotometer (Thermo Scientific, Wilmington DE, USA). Afterwards, 2 uL of RNA sample was loaded on the spectrophotometer for measurement. RNA amount was recorded at 260 nm wavelengths and RNA purity was determined by the 260/230 and 260/280 ratios. RNA was considered pure if 260/280 (RNA:protein contamination) ratio was in the range of 1.8–2.0, and 260/230 (RNA:Ethanol Contamination) was between 2.0–2.2.

cDNA synthesis

200 ng of total RNA was used to make cDNA. 2 uL of gDNase (Qiagen, Hilden, Germany) was added to 10 uL of RNA and heated at 42°C for 2 min to remove contamination by genomic DNA. Master mix (QuantiTect Reverse Transcription Kit, Qiagen, Hilden, Germany) containing reverse transcriptase enzyme and primer mix was added to each sample and run on thermocycler at 42°C for 30 min, followed by 3 min at 95°C to inactivate reaction. CDNA was stored at -20°C until qPCR analysis.

qPCR

Quantitative real-time PCR (qPCR) was carried out using QuantiTect SYBR Green PCR Kit from QIAGEN. qPCR primers were designed in house and purchased from Integrated DNA Technologies (Coralville, IA). Sequences: 18S: Fwd - GAATAATGGAATAGGACCGC, Rev - CTTTCGCTCTGGTCCGTCTT; GAPDH: Fwd - GTTTGTGAT GGGTGTGAACC, Rev - TCTTCTGAGTGGCAGTGATG; MyD88, Fwd - CAAGGCGATGAAGAAGGAC, Rev - CGCATCAGTCTCATCTTCCC; TLR4, Fwd - CAGCAGAGGAGAAAGCAT, Rev - CACCAGGAATAAAGTCTCTG. For MyD88 and TLR4 gene expression analysis, cell samples (n=2/group) were pooled prior to RNA extraction due to low cell counts. The single sample was then assayed in duplicate.

ELISA

TNF α and IL-1 β ELISAs were performed on the supernatants obtained from microglial *in vitro* treatments, using a dilution of 1:1 with buffer (R&D Systems, Minneapolis, MN, USA). The ELISA concentrations were then normalized to cell numbers per well. For analysis of Fig. 2, data from all media wells were averaged. There was no detectable signal for CD11b- cells in the IL-1 β ELISA. The detection limit for each ELISA was 5 pg/mL.

Flow Cytometric Analysis

Mice were intracardially perfused with PBS and tissues were then rapidly harvested, manually dissociated, and digested for 1 hr at 37°C with 1.5 mg/mL collagenase A (Roche Applied Science; Penzberg, Germany) and 0.40 mg/mL DNase I (Roche Applied Science). Cells from the digested tissue were then strained through a 70 μ m filter and washed with PBS. Red blood cells were lysed with ammonium/chloride/potassium (ACK) lysis buffer and then cells were counted and stained with LIVE/DEAD Aqua (Invitrogen/Life Technologies, Carlsbad, CA) in PBS. Samples were blocked in 5% rat serum, 5% mouse serum, 1% Fc Block (eBioscience, San Diego, CA) and stained for 30 min at 4°C with the following antibodies (eBioscience, San Diego, CA): CD11c PE-Cy5.5; F4/80 PE-Cy7; CD3e APC; Ly6G AF700; CD11b APC-Cy7; Ly6C V450; CD45 Qdot605; IA-IE Qdot655. Cells were analyzed on a BD™ LSR-II Flow Cytometer (BD Biosciences; Franklin Lakes, NJ) in the Duke Human Vaccine Institute Flow Research Facility and data was analyzed with FlowJo (Treestar; Ashland, OR).

Behavior

Postnatal day (PND) 85 (Fig. 4A), postnatal month (PNM) 4–13 (Fig. 3, Fig. 4B), and PNM 6–8 (Fig. 4C) Cre^{0/0} and Cre^{tg/0} mice were used for behavioral testing. ANY-maze tracking

software (Stoelting, Wood Dale, IL) recorded activity and time spent in respective zones for each behavior. Open field and elevated zero-maze behavioral data were collected using a ceiling-mounted camera. Videos were recorded and saved for analysis using ANYmaze tracking software (Stoelting, Wood Dale, IL). Behavioral data for Rotarod were hand scored.

Open Field (OF)

Mice were placed individually into a novel black box (no top) with dimensions of 40cm x 45cm x 34cm (height). Each mouse spent 30 min in the novel area. $Cre^{0/0}$ and $Cre^{tg/0}$ were alternated and tests were conducted on consecutive days at the same start time to control for time of day. Area was thoroughly cleaned with QTB and warm water after each trial to remove residual odors. ANYmaze tracking software (Stoelting, Wood Dale, IL) recorded motor activity and time spent in two zones: the center (defined as a 30×30 square) and the surrounding area.

Elevated zero maze (EZM)

Zero maze test was performed at approximately one year of age. Each mouse was placed individually into maze for 5 min. The maze was a circular metal platform with four areas: two “open arms” (platform with no walls) and two “closed arms” (platform with walls) of equal area. The platform was elevated 40 cm, with a width of 5cm and walls surrounding the closed arms at 15 cm tall. Each mouse was carried to the room containing the maze in a closed black container. The mice were placed on the platform at the intersection of the open and closed arms (alternating which closed arm). Both the maze and carrying container were thoroughly cleaned with QTB and then water between trials. During the test, total time spent in the open arms was recorded via ANYmaze and later corroborated with hand timed data.

Rotarod motor coordination (RR)

Rotarod testing occurred over three consecutive days for each mouse: an acclimation day, a training day and a test day. Testing on each day began at same time to control for time of day effects. On the acclimation day, mice were placed on the rod for 45 seconds (sec) without rotation. Then the rod was rotated for 60 sec at 4 rpm, and the mice were then returned to their cage for 15 min. After the rest period, mice were placed back on the rod at an initial speed of 4 rpm and an acceleration of 0.2 rpm/sec. The time at which each mouse fell was recorded.

On the second day (training day), three trials were performed where rod was accelerated at 0.2 rpm/sec and the time at which each mouse fell was recorded for each trial. This process was repeated on third (test) day.

Morris Water Maze (MWM)

A circular tank (122 cm diameter, 61 cm high; Med-Associates, Fairfax, VT) was filled with water (20 ± 1 °C) made opaque with the addition of white tempera paint. The platform (10 cm diameter) was placed ~30 cm away from the edge of the tank) was submerged 2 cm underneath the water surface. Visual cues were placed on walls to allow for spatial navigation. A camera wired to an EthoVision XT (ver. 9.0.722, Noldus, Wageningen, Netherlands) tracking software was used for all recordings. Analysis of latency to platform,

distance travelled, and time spent in each quadrant was performed in the Ethovision software.

MWM training occurred over four consecutive days for each mouse. Each training day consisted of three 1 min trials, each with <15 min intertrial interval, with new starting positions using a pseudo-random sequence. Mice that did not reach the platform within 1 min were guided to the platform by the experimenter and mice were allowed to rest on the platform for 15 sec. Latency to reach platform and distance travelled were recorded.

Spatial memory was assessed through two probe trials on day 5, with different starting locations for each trial. On day 5, the platform was removed and mice were given 30 sec each trial and time in each quadrant was recorded.

Conditioned place preference (CPP)

Unbiased CPP was performed similar to previously published morphine CPP paradigms (Rivera *et al*, 2015). Briefly, male PNM 4 Cre^{0/0} and Cre^{tg/0} mice were placed into a three chambered CPP box (MED-CPP-3013; Med Associates, Fairfax, VT) and allowed to move freely throughout on day 1 (pretest). Automated data collection from photo beam breaks occurred using Med-PC IV software. To configure an unbiased CPP paradigm, the individual mouse pretest CPP scores for each genotype were adjusted for an average per group closest to zero. On days 1 and 3, mice were then paired (20 min) to a previously determined non-drug context with saline, and on days 2 and 4, mice were paired to the drug context with morphine (3 mg/kg, s.c.). Any mouse with a CPP pretest score ± 240 s was automatically paired to receive drug in the non-preferred context, and received pairing along with other cage mates; however these data were not included in the analysis. After pairing, mice rested in home cages for 48h until day 8 when a 30 min test was performed with no drug onboard. For subsequent tests, a positive CPP score (i.e. reward) indicates a greater number of seconds spent in the morphine-paired chamber compared to the saline paired chamber. The opposite is also true, if a negative CPP score (i.e. aversion) is observed then a greater number of seconds were spent in the saline-paired chamber compared to the morphine-paired chamber.

Extinction

Twenty-four hrs after test day, three daily extinction trials that consisted of a 20 min sequestration in the drug context without drug onboard (D9–11) and on day 12 a 30 min extinction test was performed (Schwarz *et al*, 2011). Mice were allowed to rest for 72 hrs before the next extinction trials and testing was performed. The overall extinction paradigm was performed over 7 weeks.

Reinstatement

Unintended contextual cues, such as the experimenter, handling, environment, and injection during drug delivery may contribute to a conditioned response and therefore elicit reinstatement behavior (Bardo and Bevins 2000). In addition, saline administration has been shown to increase stress-related behaviors and physiology in rats (Saldívar-González, Arias, and Mondragón-Ceballos 1997; Stone and John 1992). Therefore, if reinstatement is not

observed after administration of saline (Portugal et al. 2014; Zhao et al. 2017), then the subsequent drug-induced reinstatement is believed to be due to the rewarding stimuli using a low dose of morphine. Furthermore, a saline injection is not expected to elicit reinstatement as the memory encoded from repeated exposure to the context requires the rewarding drug (Lee et al. 2015). After 7 weeks of extinction training, reinstatement to saline and morphine occurred by s.c. administered saline (D60) or morphine (D61) and mice were allowed to freely move throughout the CPP box for 30 min. Mice were sacrificed 24 hrs after morphine reinstatement.

Immunohistochemistry (IHC)

For *Cx3cr1-CreBT:Rosa26-tdTomato*, *Rosa26-DTR*, and *Cx3cr1-CreBT:DTR* mice in Figs. 1–2, tissue was extracted and cryoprotected in 30% sucrose with 0.1% sodium azide. Tissue was then sectioned using a cryostat at 25 μ m. In Fig. 1, Sections from *Rosa26-DTR*, and *Cx3cr1-CreBT:DTR* mice were immunostained with rat-anti-CD11b (Bio-Rad, Hercules, California, U.S.A.) for 24 hrs. Secondary antibody (biotinylated-Donkey-anti-Rat, Jackson ImmunoResearch, West Grove, PA) incubated for 1 hr, and amplification (VECTASTAIN® Elite® ABC-HRP Kit, Vector Labs, Burlingame, CA) was visualized using 3,3'-Diaminobenzidine (DAB, Millipore-Sigma, Darmstadt, Germany). Slides were dehydrated/defatted with ethanol and xylene and coverslipped with DPX mountant (Merck, Darmstadt, Germany). In Fig 2A. sections from *Cx3cr1-CreBT:Rosa26-tdTomato* mice were immunostained with Goat-anti-Iba-1 (Novus Biologicals, Centennial, CO) and AlexaFlour-568 -Donkey-anti-Goat (Thermo Fisher Scientific, Waltham, MA) secondary antibody. Tissue was stained with DAPI and the endogenous tdtomato signal was visualized. The processed tissue was then coverslipped with Vectashield with DAPI (Vector Laboratories, H-1200) mountant.

For $Cre^{tg/0}$ and $Cre^{0/0}$ mice (Fig. 5 & 6), brain sectioning and IHC were performed as previously described (Rivera *et al*, 2015). Primary antibodies (Rabbit-anti-Ki67, Abcam, Cambridge, MA; Goat-anti-DCX, Santa Cruz Biotechnology, Dallas, TX; and Rabbit-anti-CD68, Abcam, Cambridge, MA) incubated for 24 hrs and then secondary antibodies (biotinylated-Horse-anti-Goat, Vector Labs, Burlingame, CA; AlexaFlour-647 -Donkey-anti-Rabbit, Thermo Fisher Scientific, Waltham, MA) were incubated for 2 hrs. Amplification of Ki67 and DCX was visualized by DAB (Fig. 5) or tyramide signal amplification (Fig. 6, Perkin Elmer, Waltham, MA). Slides were dehydrated/defatted and coverslipped with DPX mountant (Millipore-Sigma, Darmstadt, Germany) and stored at room temperature in the dark box until imaging.

For co-culture experiments (Fig. 8), round coverslips were rinsed twice with 1XPBS, blocked (5% Normal horse serum in PBS, Vector Labs, Burlingame, CA), and primary antibodies with blocking buffer (Mouse-anti-CD68, Abcam, Cambridge, MA; Goat-anti-DCX, Santa Cruz Biotechnology, Dallas, TX; and Rabbit-anti-Iba1, Wako) were incubated for 1 hr. Wells were washed with PBS and secondary antibodies (biotinylated-Goat-anti-Mouse, Vector Labs, Burlingame, CA; AlexaFlour-568 -Donkey-anti-Goat, Thermo Fisher Scientific, Waltham, MA; and 647-Donkey-anti-Rabbit, Thermo Fisher Scientific, Waltham, MA) were incubated for 1 hr. Amplification (VECTASTAIN® Elite® ABC-HRP Kit, Vector

Labs, Burlingame, CA) of CD68 was visualized by tyramide signal amplification (Perkin Elmer, Waltham, MA). Round glass coverslips were placed onto slides and were coverslipped with VectaShield™ (Novus Biologicals, Littleton, CO) aqueous mounting medium, sealed with nailpolish, and stored at room temperature in the dark box until imaging.

Image Analysis

All images were collected using a Nikon Eclipse 80i fluorescent microscope (at 100X magnification) unless otherwise noted.

Doublecortin (DCX) and Ki67 Analysis

Stacks of 10 μm DCX and Ki67 sections were collected (1 μm steps at 200X; 400X for inset images (Fig. 5); Zeiss Apotome, Oberkochen, Germany) using optical sectioning from 4–5 sections across Bregma -1.2 to -3.4 mm. Subtract background and thresholding (OTSU) were applied to all stacks using ImageJ software (ver. 1.51j8, NIH, USA). ROIs were manually drawn around either the granule cell layer (GCL) of the dentate gyrus (DG) for DCX or the subgranular zone (SGZ) of the DG for Ki67. The SGZ region is defined as half way into the GCL and two cell widths into the hilar region of the DG. Max projections of the stacks were taken and the integrated density (ID) measurements of Ki67 and DCX signal were taken from within ROI of the SGZ or GCL, respectively.

DCX, CD68, and Iba-1 Image Analysis

Stacks of 10 μm DCX, CD68, and Iba-1 cells were collected (1 μm steps at 200X; Zeiss Apotome, Oberkochen, Germany) using optical sectioning from 3 image fields. Subtract background and thresholding (DCX and CD68, OTSU; Iba-1, Moments) were applied to all stacks using ImageJ software (ver. 1.51j8, NIH, USA).

3D-Reconstructions

All GCL DG ROI stacks, from Bregma -1.2 to -3.4 mm, were obtained using a Nikon A1SiR confocal microscope (Melville, NY). Subtract background and thresholding (OTSU) were applied to all stacks using ImageJ software and ROIs were manually drawn around the granule cell layer (GCL) of the dentate gyrus (DG). Stacks of merged and split channels for CD68 and DCX were imported into Imaris software (ver. 8.3.1, Bitplane, Zurich, Switzerland) and the 3D-reconstructions for single (DCX, voxel=1.0; CD68, voxel=10) and colocalization (voxel = 1) channels were built from threshold values determined by ImageJ software (CD68, OTSU; DCX, OTSU). Surface area values of all 3D reconstructions were then divided by the volume from each ROI DG GCL z-stack obtained. To calculate the colocalization within the DCX and CD68 surface volumes, the colocalized surface volume value was divided by the CD68 and DCX surface volume values. In doing so, only the positive signal from CD68 and DCX found within the DG was examined, thereby removing the negative space from the colocalization calculation (Fig. 7A-F). For the co-culture experiment, 3D-reconstructions for the colocalization channel was built from threshold values determined by ImageJ software (CD68, OTSU; DCX, OTSU; Iba-1, Moments, Fig. 8).

Experimental Design and Statistical Analysis

Graphpad (PRISM) software was used for Pearson's correlations, Student's *t*-tests, one- and two-way Analysis of Variance (ANOVA). Repeated measures (RM) analysis are indicated when used. Post-hoc analysis used the Holm-Sidak for RM analysis or Tukey's multiple comparison (Aickin and Gensler, 1996). Statistical significance (α) was defined as $P < 0.05$.

Results

Cx3cr1-CreBT^{tg/0} mice precisely label and disrupt parenchymal microglia within the CNS.

Previous knock-in studies show that *CX3CR1* knockdown (i.e. in heterozygote mice) can impact neurogenesis, microglial activation, and microglial cell numbers during development. Therefore, *Cx3cr1-CreBT* mice were developed to ensure *Cx3cr1* locus function remains intact. To establish a proof of concept that *Cx3cr1-CreBT* mice can be used for Cre-mediated gene targeting in resident monocytes and tissue macrophage populations, *Cx3cr1-CreBT:DTR* (diphtheria toxin receptor expressing) mice were treated with diphtheria toxin (DT, 150 ng/g, *i.p.* daily for 3 days). DT-treated *Cx3cr1-Cre:DTR* mice demonstrated a dramatic reduction in parenchymal CD11b⁺ microglia while control mice (*Rosa26-DTR*) were unaffected by DT treatment (Fig. 1).

Next, histology of *Cx3cr1-CreBT:tdTomato^{f/wt}* reporter mice brains were used to label all CreBT⁺ cells (Madisen et al. 2010). In the brains of *Cx3cr1-CreBT:tdTomato^{f/wt}* mice, all parenchymal microglia expressed tdTomato in a pattern that overlapped staining for Iba-1, a ubiquitous calcium-binding adaptor protein expressed on microglia (Fig. 2A). No tdTomato expression was observed in non-myeloid populations, including neurons, astrocytes, and oligodendrocytes. In *Cx3cr1-CreBT:tdTomato^{f/wt}* mice, tdTomato was expressed in patterns consistent with those of liver Kupffer cells, splenic red pulp macrophages, and lung alveolar macrophages (not shown). These results are very similar to published "knock-in" *Cx3cr1-Cre* mouse models (Jung et al. 2000; Yona et al. 2013) and establish the proof of concept that *Cx3cr1-CreBT* mice can be used for Cre-mediated gene targeting in resident monocytes and tissue macrophages, without affecting *Cx3cr1* locus function.

Cx3cr1-CreBT^{tg/0}:MyD88^{ff} microglia have a diminished pro-inflammatory response.

To determine the parenchymal microglial response from *Cx3cr1-CreBT:MyD88^{ff}* mice, CD11b⁺ (microglia) and CD11b⁻ cells (astrocytes, neurons, oligodendrocytes, and other non-microglial cells) were isolated from whole brain homogenates of WT, Cre^{0/0}, and Cre^{tg/0} mice. RT-qPCR on CD11b⁺ cells revealed similar levels of *MyD88* gene expression in WT and Cre^{0/0} mice, while Cre^{tg/0} mice have downregulated *MyD88* levels, compared to WT and Cre^{0/0} controls. CD11b⁻ cells showed no difference in *MyD88* gene expression levels, across all genotypes (Fig. 2B). To assess the innate inflammatory response in WT, Cre^{0/0}, and Cre^{tg/0} mice, lipopolysaccharide (LPS, 10 ng/mL) was given to CD11b⁺ cultures and ELISAs for IL-1 β and tumor necrosis factor-alpha (TNF α), were performed on CD11b⁺ cells isolated from WT, Cre^{0/0}, and Cre^{tg/0} brains with and without LPS treatment; IL-1 β was significantly increased after LPS treatment in both Cre^{0/0} and WT mice (Interaction, $F(2,12)=12.96$, $P < 0.001$), while IL-1 β was not detected (N.D.) in Cre^{tg/0} mice (Fig. 2C);

TNF α was significantly increased after LPS treatment in Cre^{0/0} mice compared to Cre^{tg/0} mice (Fig. 2D, Interaction, F(2,6)=6.21, $P<0.05$). IL-1 β and TNF α levels from isolated CD11b⁺ cells were either N.D. or negligible (data not shown).

Mice with depleted MyD88 from microglia have normal acquisition, prolonged extinction, and enhanced reinstatement of a morphine reward memory.

Whole-body knockout (KO) mice of *TLR4* and *MyD88* have previously shown an inability to acquire an oxycodone/context association (M. R. Hutchinson et al. 2012). Briefly, morphine binds directly to MD-2, a critical adaptor protein necessary for TLR4 downstream signaling and cytokine production (M. R. Hutchinson et al. 2012; Mark R. Hutchinson et al. 2010; Wang et al. 2012). Therefore, mCPP was performed on Cre^{0/0} and Cre^{tg/0} mice to examine acquisition, extinction, and reinstatement of a drug/context association (Fig. 3A) using a low dose of morphine (3 mg/kg). Mice from both Cre^{0/0} and Cre^{tg/0} genotypes had higher CPP scores on test day (repeated measures two-way ANOVA, main effect of time (F(1,11)=37.62, $P<0.01$)) compared to pretest scores (Fig. 3B; $P_s<0.05$). Extinction CPP scores showed a main effect of Extinction Trials (F(7,77)=7.065) and Genotype (F(1,11)=5.753, $P_s<0.05$), and no significant interaction (F(7,77)=1.259) by repeated measures two-way ANOVA (Fig. 3C). However, Cre^{tg/0} had a higher average extinction CPP score compared to Cre^{0/0} (Fig. 3D; Student's *t*-test, $P<0.05$). Aversion was examined across extinction trials by repeated measures two-way ANOVA comparison of extinction trials to the pretest CPP scores. We found a main effect of Time (F(8,88)=6.641) and Genotype (F(8,88)=6.371, $P_s<0.05$), but no significant interaction (F(8,88)=1.325; data not shown). No significant post-hoc analyses or Student's *t*-tests were found when comparing the pretest CPP score to any extinction trials.

Drug-, stress-, or cue-induced reinstatement of an acquired drug/context association is considered a model for drug-, stress-, or cue-induced craving in abstinent humans that can lead to drug-taking behavior (i.e. relapse) (Tzschentke 2007). Unintended contextual cues (see SI material)-induced reinstatement, assessed by administration of saline (s.c.), did not impact reinstatement CPP scores in Cre^{0/0} or Cre^{tg/0} genotypes. However, drug-induced (priming dose of 3 mg/kg morphine, s.c.) reinstatement CPP scores (main effect of Genotype (F(1,11)=5.003; $P<0.05$)) were higher in Cre^{tg/0}-morphine mice compared to Cre^{tg/0}-Extinction Trial #7 (*t*-test, $P=0.058$) (Fig. 3E), while no differences were observed in Cre^{0/0} mice.

Mice lacking microglial MyD88 display normal behaviors for anxiety, locomotion, and learning and memory.

CPP is an indirect measure of drug seeking behavior and the interpretation can be complicated by changes in co-morbid behaviors, including anxiety and activity. To determine if ablated microglial-*MyD88* signaling during development affects general behavior, anxiety-like behavior in the open field (OF, PND 85) (time in center vs. surround) was assessed on PND85 (Fig. 4A). No difference by genotype was observed (Fig. 4A₁). A separate group of *Cx3cr1-CreBT:MyD88^{fl/fl}* mice was allowed to age to 4 months (PNM 4), a time point in which we assessed neurogenesis, and used to examine anxiety-like behaviors using OF and EZM at PNM 11. Rotarod (PNM 13) was also used to examine motor

coordination (Fig. 4B). No differences in any measure were observed between Cre^{0/0} or Cre^{tg/0} genotypes (Fig. 4B₁₋₄), at any age.

Finally, because a specific change in extinction learning during CPP in Cre^{tg/0} mice was observed, non-morphine associated learning and memory was assessed in a separate group by Morris Water Maze (MWM, Fig. 4C) to compare microglia deficient in MyD88 signaling to previously published literature that suggested whole-body depletion of TLR4 enhanced memory retention for water maze and contextual fear memory (Okun et al. 2012). No differences in latency to find the platform or the distance travelled were observed between Cre^{0/0} or Cre^{tg/0} genotypes across training days (Fig. 4C_{1,2}). During the probe test, both genotypes also spent significantly more time in the target quadrant compared to other quadrants (Fig. 4C₃), demonstrating equivalent learning and memory in this non-drug contingent paradigm.

Depletion of MyD88 from microglia differentially impacts markers of adult neurogenesis in the hippocampal dentate gyrus after morphine CPP.

One recently discovered role for AHNG is to aid in extinction learning, or new inhibitory learning, of cocaine CPP (Castilla-Ortega et al. 2016). We determined if naïve Cre^{tg/0} (PND 120) mice had altered AHNG by examining the proliferative and immature neuronal population labeled by Ki67 (Fig. 5A) and doublecortin, DCX (Fig. 5D), respectively. Under physiological conditions, drug-naïve mice had no differences in the integrated density (i.e. sum of pixel values, assessed by ImageJ) of Ki67 (Fig. 5B) or DCX (Fig. 5E). After mCPP, both genotypes showed a general reduction of Ki67 and DCX compared to naïve mice, suggesting that the mCPP paradigm, or potentially morphine alone, was necessary to diminish overall levels of AHNG in the DG hippocampus, consistent with previous studies (Eisch et al. 2000; Arguello et al. 2009). However, Cre^{tg/0} mice showed significantly greater integrated density of DG DCX ($P < 0.05$, Student's *t*-test), compared to Cre^{0/0} mice, after mCPP (Fig. 5F), while Ki67 remained unchanged (Fig. 5C). Taken together, these data suggest that MyD88 deletion in microglia impacts the maturation, but not proliferation, of new born neurons, following mCPP.

MyD88-deficient mice show increased immature neuronal debris inside microglial lysosomes only after morphine CPP.

Previous research demonstrates a critical role for microglial phagocytosis in the removal of extraneous newborn neurons within the healthy adult DG (Sierra et al. 2010). To test whether altered microglia in our mice had evidence of altered elimination of DCX cells in the DG of Cre^{tg/0} mice after morphine, lysosomal volumes in microglial cells were examined (von Bernhardi, Eugenín-von Bernhardi, and Eugenín 2015; Floden and Combs 2011) by creating 3D-reconstructions of CD68, a lysosomal marker found in microglia, and DCX in the DG GCL of the hippocampus (Fig. 6A). In naïve mice, CD68, DCX, and colocalized CD68+DCX+ surface volumes, normalized to the total DG volume, showed no differences between Cre^{0/0} and Cre^{tg/0} genotypes. In contrast, after mCPP testing, CD68 (*t*-test, [#] $P = 0.0601$) and colocalized surface volumes (normalized to the total DG volume, *t*-test, $P < 0.05$) were increased in Cre^{tg/0} compared to Cre^{0/0} mice, while no difference in DCX total surface volumes was found (Fig. 7).

Similarly, when the amount of colocalized surface volumes (Fig. 7C) was normalized to total CD68⁺ (Fig. 7A) and DCX⁺ (Fig. 7B) surface volumes within the DG, drug-naïve mice showed no difference between Cre^{0/0} and Cre^{tg/0} genotypes (Fig. 6B). However, after mCPP, there was a significant increase ($P<0.05$) in the amount of colocalized surface volumes in Cre^{tg/0} mice, compared to Cre^{0/0} controls, by Student's *t*-test (Fig. 6C).

To further examine the impact of microglial-MyD88 signaling on immature neuron engulfment in response to morphine, Cre^{0/0} and Cre^{tg/0} mice were acutely treated *in vivo* with saline or morphine, and primary cell co-cultures of immature neurons (PSA-NCAM) and microglia (CD11b, Fig. 8A) were prepared 1 hr later. Microglia were allowed to “feed” on neurons in culture for 1 hr, and cells were fixed and stained for DCX, CD68, and Iba1, and the DCX/CD68 colocalization volume within Iba1+ cells were calculated and analyzed. We found a significant genotype by treatment interaction by two-way ANOVA ($F(1,7)=7.797$, $P<0.05$, Fig. 8); post hoc analysis showed that Cre^{tg/0} mice have a significant increase in the colocalized surface volume amount only after morphine, compared to Cre^{0/0} controls (Student's *t*-test, $P<0.05$), consistent with our *in vivo* data (Fig. 6C). These data support our conclusions that intact microglial-MyD88 signaling is critical for microglial immature neuron engulfment (and potential degradation, though this remains to be directly determined), but only after a morphine challenge.

Amount of CD68⁺ and DCX⁺ colocalization positively correlates with CPP scores during extinction.

Together, the present data indicate that after mCPP, diminished microglial-*MyD88* signaling results in prolonged extinction of a morphine reward memory (Fig. 3D), increased DCX staining in the DG (Fig. 5F), and an increase in the amount of colocalization of CD68⁺DCX⁺ cells following drug re-exposure (Fig. 6C). To further explore these findings, a Pearson's correlation was used against the amount of colocalization of CD68⁺DCX⁺ and CPP score across the CPP paradigm to determine which stages of CPP are associated with the increased colocalization of CD68 and DCX (data not shown). No significant correlation between colocalization amount in the Pretest ($R^2=0.03$, $P=0.6$) or Test ($R^2=0.185$, $P=0.187$) was observed. However, significant positive correlations between colocalized amount and CPP scores in extinction trial 3 ($R^2=0.442$, $P=0.025$) and 4 ($R^2=0.447$, $P=0.024$), were observed, along with a trend towards significance in the drug-induced reinstatement of mCPP ($R^2=0.327$, $P=0.066$). Our data suggest that deletion of *MyD88* signaling within microglia can result in increased lysosomal volumes, which correlates with prolonged extinction and higher reinstatement following morphine administration in Cre^{tg/0} mice. This is consistent with previous data showing an important role for glial inflammatory response in reinstatement, but not the initial acquisition of mCPP (Schwarz, Hutchinson, and Bilbo 2011). Taken together, these data highlight a surprising protective effect of microglial-*MyD88* neuro-immune signaling in the face of opioid exposure.

Discussion

We report that enhancement of addiction-like behaviors (i.e. prolonged extinction and enhanced reinstatement) coincided with aberrant DCX levels in Cre^{tg/0} compared to Cre^{0/0}

mice after mCPP. We also determined that the amount of colocalized surface volumes of microglial lysosomes (CD68) and DCX of Cre^{tg/0} mice was increased compared to Cre^{0/0} mice only after mCPP. Interestingly, there was a positive correlation between the colocalized surface volumes of DCX and CD68 and the CPP score during the extinction trials. Thus, the data do not support our original hypothesis that a depletion of neuro-immune signaling specifically from microglia would abolish the retrieval of a morphine/context association, similar to whole-body knockouts of immune related signaling targets. Rather, these data support a novel protective role for microglial *MyD88* signaling in reward learning and maintenance, which has important implications for the development of glial-targeted therapies for addiction.

Diminished microglial-MyD88 signaling enhances persistence of rewarding behaviors

Our most interesting finding is that intact microglial-*MyD88* signaling, using a low dose of morphine, lends normal acquisition to mCPP, facilitated the extinction of the reward memory, and may potentially prevent reinstatement to morphine. First, in regards to acquisition of morphine CPP, our finding is opposite of whole-body knockouts of *TLR4* and *MyD88* (M. R. Hutchinson et al. 2012) as well as the pharmacological blockade of *TLR4* by (+)-naloxone, which show disrupted acquisition of (+)oxycodone CPP (M. R. Hutchinson et al. 2012).

Furthermore, minocycline, a glial cell modulator that inhibits glial cell proinflammatory function, can inhibit acquisition to mCPP (Mark R. Hutchinson et al. 2008) when given prior to testing/training, supporting a role for activated glial cells mediating the acquisition of rewarding addiction-like behaviors. Notably, the lack of acquisition in each of these paradigms makes it difficult to evaluate the role of microglial signaling in specific aspects of addiction pathology, e.g. acquisition vs extinction. Several studies have examined the impact of using immunomodulators (i.e. (+)-naltrexone and minocycline) on extinction and reinstatement by administering them after acquisition of a rewarding memory. For example, administration of immunomodulators during withdrawal can lead to diminished addiction-like behaviors such as lower response rates to cocaine SA (Northcutt et al. 2015), decreased development of heroin craving after SA (Theberge et al. 2013), and attenuated reinstatement to methamphetamine (Attarzadeh-Yazdi, Arezoomandan, and Haghparast 2014) and morphine (Arezoomandan, Khodaghali, and Haghparast 2016) CPP. Taken together, these data must be interpreted in the light that each of these immunomodulators and whole-body knockout mice impact microglia, neurons, and many other cell types responsible for the induction and maintenance of a rewarding memory. Our data uniquely suggests that intact neuro-immune signaling specifically from microglia may be required for normal extinction and in the prevention of reinstatement to morphine after CPP training. This said, while our mouse model achieves a higher degree of cell specificity, we recognize a potential role for peripheral monocytes/macrophages to have an impact in the observed results.

Intact neuro-immune signaling after mCPP alters DCX levels

Under physiological conditions, previous murine whole-body knockout studies of *TLR4* and *MyD88* (Rolls et al. 2007) genes, found in many CNS cell types (Ye Zhang et al. 2014), show an *increase* in DG AHNG. Similarly, in an animal model of stroke, chronic

administration of minocycline, but not vehicle controls, increased the number of new adult neurons produced in the DG (Liu et al. 2007). In the present study and under physiological conditions, naïve Cre^{tg/0} mice exhibit normal behavior and have no difference in Ki67 or DCX compared to Cre^{0/0} control mice. Therefore, we suspect that microglial-specific neuro-immune signaling during physiological conditions is not directly involved in a general increase of AHNG. In agreement with previous studies using chronic morphine and mCPP (Yue Zhang et al. 2016; Arguello et al. 2008), a decrease in Ki67 and DCX levels in Cre^{0/0} mice is observed, when qualitatively compared to naïve Cre^{0/0} mice. The results also indicate that the mCPP paradigm increased DCX in Cre^{tg/0} mice, when compared to Cre^{0/0} mice, while Ki67 remained unchanged. These data agree with previously published data that correlate deficits in spatial memory, social memory, and in stress coping with modest reductions of DCX in rodents (Garrett et al. 2015; Lagace et al. 2010; Jessberger et al. 2009). One possible interpretation of these data is that microglial neuro-immune signaling is an important extrinsic factor in the appropriate removal of surviving and maturing newborn neurons, and not the proliferative precursors, after mCPP. Taken together, whole-body knockout mice of neuro-immune signaling components appear to constitutively impact DCX, while microglial-specific regulation of DCX relies on perturbations to the CNS.

Impaired DCX and increased microglial lysosomal volumes may alter drug reward memories

Diminishing or ablating AHNG prior to a rewarding behavior increases drug intake after morphine (Bulin et al. 2017) and cocaine SA (Noonan et al. 2010), and prolongs extinction of cocaine CPP (Castilla-Ortega et al. 2016). We observed a similar prolonged extinction of mCPP by depleting microglial-*MyD88* signaling. As immune modulation can influence learning and memory and AHNG (Yirmiya and Goshen 2011; Rogers et al. 2011; Liu et al. 2007), it is not surprising that neuro-immune signaling can play a homeostatic role in cognition. For example, the cytokine TNF α is known to have both protective and detrimental effects in the brain (review (Sriram and O'Callaghan 2007)). Given the role of AHNG on reward behaviors such as CPP, we explored if and how microglia might interact with cells important for the extinction of a reward-context associated memory (Castilla-Ortega et al. 2016) by examining microglial lysosomal volumes and their contents.

The observed increase in colocalized CD68 and DCX surface volumes in Cre^{tg/0} mice may represent a dysfunction of lysosomal activity or debris elimination, compared to Cre^{0/0} controls. This possibility remains to be tested directly but is supported by the observation in *ex vivo* cultures of increased DCX+CD68+Iba1+ colocalized surface volumes from Cre^{tg/0} mice treated acutely *in vivo* with morphine, compared to Cre^{0/0} controls. Proper microglial phagocytic activity, via lysosomes, is mediated by the Rag-Ragulator complex in zebrafish microglia (Shen, Sidik, and Talbot 2016). Importantly, microglial phagocytosis is conserved from invertebrates to vertebrates and impairments are associated with neurodevelopmental (Kim et al. 2016; Shen, Sidik, and Talbot 2016) and neurodegenerative disorders (Fiala et al. 2005). For example, in humans with Alzheimer's disease, impairments in microglial phagocytosis of amyloid beta (A β) plaques have also been observed (Fiala et al. 2005). Furthermore, murine whole-body knockouts of *MyD88* and *Cx3cr1* show impairments in microglial phagocytosis of A β plaques (Michaud, Richard, and Rivest 2012). Whether

through dysregulated phagocytosis or lysosomal activity, the present study provides novel evidence that microglial specific neuro-immune *MyD88* signaling is important in the maintenance of immature neurons after morphine, which may subsequently impact addiction-like behaviors.

Conclusions

Taken together, these data suggest that diminished microglial MyD88 neuro-immune signaling increased microglial lysosomal volumes containing DG DCX debris, correlating with prolonged extinction and enhanced reinstatement of a reward memory. In the current manuscript, the MyD88 protein was deleted in monocytes and macrophages, but lacks a gain-of-function experiment, thus caution must be taken to interpret the results of this study. It should be noted that the changes we observed in the DG of the hippocampus are undoubtedly part of a larger circuit, which we look forward to examining in future experiments. Overall, this work expands our knowledge of neuro-immune signaling as an important component in the learning and memory processes involved in addiction. Therefore, a better understanding of microglia-specific signaling should also be examined in the future, as novel microglia-specific treatments may aid those to overcome substance use disorders.

Acknowledgments

We thank Dr. Marcy Kingsbury for the use of her Zeiss microscope. We thank the NIDA Research Resources Drug Supply Program for the morphine sulfate provided for these studies. Author contributions: PDR, MJK, RH, SDB, and MG contributed to the experimental design, data interpretation, and wrote the manuscript. PR, MJK, RH, PKT, and DS performed molecular and behavioral experiments. YCJ and PR performed 3D reconstructions and data analysis. All authors discussed and commented on the manuscript.

Funding and Disclosure

This work was supported by grants from NIH/NIDA (DA034185) to SDB. PDR was supported by NIDA (DA034185-03S1 to SDB). The authors declare no conflict of interest.

References

- Aickin Mikel, Gensler Helen. (1996). "Adjusting for multiple testing when reporting research results: the Bonferroni vs Holm methods." *American Journal of Public Health* 86: 726–728. [PubMed: 8629727]
- Arezoomandan Reza, Khodaghali Fariba, and Haghparast Abbas. 2016 "Administration of the Glial Condition Medium in the Nucleus Accumbens Prolong Maintenance and Intensify Reinstatement of Morphine-Seeking Behavior." *Neurochemical Research* 41 (4): 855–68. [PubMed: 26547198]
- Arguello AA, Fischer SJ, Schonborn JR, Markus RW, Brekken RA, and Eisch AJ. 2009 "Effect of Chronic Morphine on the Dentate Gyrus Neurogenic Microenvironment." *Neuroscience* 159 (3): 1003–10. [PubMed: 19356684]
- Arguello AA, Harburg GC, Schonborn JR, Mandyam CD, Yamaguchi M, and Eisch AJ. 2008 "Time Course of Morphine's Effects on Adult Hippocampal Subgranular Zone Reveals Preferential Inhibition of Cells in S Phase of the Cell Cycle and a Subpopulation of Immature Neurons." *Neuroscience* 157 (1): 70–79. [PubMed: 18832014]
- Attarzadeh-Yazdi Ghassem, Arezoomandan Reza, and Haghparast Abbas. 2014 "Minocycline, an Antibiotic with Inhibitory Effect on Microglial Activation, Attenuates the Maintenance and Reinstatement of Methamphetamine-Seeking Behavior in Rat." *Progress in Neuro-Psychopharmacology & Biological Psychiatry* 53 (August): 142–48. [PubMed: 24768984]

- Bachstetter Adam D., Morganti Josh M., Jernberg Jennifer, Schlunk Andrea, Mitchell Staten H., Brewster Kaelin W., Hudson Charles E., et al. 2011 “Fractalkine and CX 3 CR1 Regulate Hippocampal Neurogenesis in Adult and Aged Rats.” *Neurobiology of Aging* 32 (11): 2030–44. [PubMed: 20018408]
- Bachtell Ryan K., Jones Jermaine D., Heinzerling Keith G., Beardsley Patrick M., and Comer Sandra D. 2017 “Glial and Neuroinflammatory Targets for Treating Substance Use Disorders.” *Drug and Alcohol Dependence* 180 (August): 156–70. [PubMed: 28892721]
- Bardo MT, and Bevins RA. 2000 “Conditioned Place Preference: What Does It Add to Our Preclinical Understanding of Drug Reward?” *Psychopharmacology* 153 (1): 31–43. [PubMed: 11255927]
- Bernhardi Rommy von, Laura Eugenín-von Bernhardi, and Jaime Eugenín. 2015 “Microglial Cell Dysregulation in Brain Aging and Neurodegeneration.” *Frontiers in Aging Neuroscience* 7 (July): 124. [PubMed: 26257642]
- Bolós M, Perea JR, Terreros-Roncal J, Pallas-Bazarrá N, Jurado-Arjona J, Ávila J, and Llorens-Martín M. 2017 “Absence of Microglial CX3CR1 Impairs the Synaptic Integration of Adult-Born Hippocampal Granule Neurons.” *Brain, Behavior, and Immunity*, 10 10.1016/j.bbi.2017.10.002.
- Bulin Sarah E., Mendoza Matthew L., Richardson Devon R., Song Kwang H., Solberg Timothy D., Yun Sanghee, and Eisch Amelia J. 2017 “Dentate Gyrus Neurogenesis Ablation via Cranial Irradiation Enhances Morphine Self-Administration and Locomotor Sensitization.” *Addiction Biology*, 6 10.1111/adb.12524.
- Castilla-Ortega Estela, Blanco Eduardo, Serrano Antonia, de Guevara-Miranda David Ladrón, Pedraz María, Estivill-Torrús Guillermo, Pavón Francisco Javier, de Fonseca Fernando Rodríguez, and Santín Luis J. 2016 “Pharmacological Reduction of Adult Hippocampal Neurogenesis Modifies Functional Brain Circuits in Mice Exposed to a Cocaine Conditioned Place Preference Paradigm.” *Addiction Biology* 21 (3). Wiley Online Library: 575–88. [PubMed: 25870909]
- Eisch AJ, Barrot M, Schad CA, Self DW, and Nestler EJ. 2000 “Opiates Inhibit Neurogenesis in the Adult Rat Hippocampus.” *Proceedings of the National Academy of Sciences of the United States of America* 97 (13): 7579–84. [PubMed: 10840056]
- Ferbinteanu J, and McDonald RJ. 2001 “Dorsal/ventral Hippocampus, Fornix, and Conditioned Place Preference.” *Hippocampus* 11 (2): 187–200. [PubMed: 11345125]
- Fiala Milan, Lin Justin, Ringman John, Kermani-Arab Vali, Tsao George, Patel Amish, Lossinsky Albert S., et al. 2005 “Ineffective Phagocytosis of Amyloid- β by Macrophages of Alzheimer’s Disease Patients.” *Journal of Alzheimer’s Disease: JAD* 7 (3). IOS Press: 221–32. [PubMed: 16006665]
- Floden Angela Marie, and Combs Colin Kelly. 2011 “Microglia Demonstrate Age-Dependent Interaction with Amyloid- β Fibrils.” *Journal of Alzheimer’s Disease: JAD* 25 (2): 279–93.
- Garrett L, Zhang J, Zimprich A, Niedermeier KM, Fuchs H, Gailus-Durner V, Hrab de Angelis M, Vogt Weisenhorn D, Wurst W, Hölter SM, 2015 Conditional Reduction of Adult Born Doublecortin-Positive Neurons Reversibly Impairs Selective Behaviors. *Front. Behav. Neurosci* 9, 302. [PubMed: 26617501]
- Hutchinson Mark R., Northcutt Alexis L., Chao Lindsey W., Kearney Jeffrey J., Zhang Yingning, Berkelhammer Debra L., Loram Lisa C., et al. 2008 “Minocycline Suppresses Morphine-Induced Respiratory Depression, Suppresses Morphine-Induced Reward, and Enhances Systemic Morphine-Induced Analgesia.” *Brain, Behavior, and Immunity* 22 (8): 1248–56.
- Hutchinson Mark R., Zhang Yingning, Shridhar Mitesh, Evans John H., Buchanan Madison M., Zhao Tina X., Slivka Peter F., et al. 2010 “Evidence That Opioids May Have Toll-like Receptor 4 and MD-2 Effects.” *Brain, Behavior, and Immunity* 24 (1): 83–95.
- Hutchinson MR, Northcutt AL, Hiranita T, Wang X, Lewis SS, Thomas J, van Steeg K, et al. 2012 “Opioid Activation of Toll-like Receptor 4 Contributes to Drug Reinforcement.” *The Journal of Neuroscience: The Official Journal of the Society for Neuroscience* 32 (33): 11187–200. [PubMed: 22895704]
- Jessberger S, Clark RE, Broadbent NJ, Clemenson GD, Consiglio A, Lie DC, Squire LR, Gage FH, 2009 Dentate gyrus-specific knockdown of adult neurogenesis impairs spatial and object recognition memory in adult rats. *Learn. Mem* 16, 147–154. [PubMed: 19181621]

- Jung S, Aliberti J, Graemmel P, Sunshine MJ, Kreutzberg GW, Sher A, and Littman DR. 2000 "Analysis of Fractalkine Receptor CX(3)CR1 Function by Targeted Deletion and Green Fluorescent Protein Reporter Gene Insertion." *Molecular and Cellular Biology* 20 (11): 4106–14. [PubMed: 10805752]
- Kim H-J, Cho M-H, Shim WH, Kim JK, Jeon E-Y, Kim D-H, and Yoon S-Y. 2016 "Deficient Autophagy in Microglia Impairs Synaptic Pruning and Causes Social Behavioral Defects." *Molecular Psychiatry*, 7 Nature Publishing Group. 10.1038/mp.2016.103.
- Lacagnina Michael J., Kopec Ashley M., Cox Stewart S., Hanamsagar Richa, Wells Corinne, Slade Susan, Grace Peter M., Watkins Linda R., Levin Edward D., and Bilbo Staci D.. 2017 "Opioid Self-Administration Is Attenuated by Early-Life Experience and Gene Therapy for Anti-Inflammatory IL-10 in the Nucleus Accumbens of Male Rats." *Neuropsychopharmacology: Official Publication of the American College of Neuropsychopharmacology* 42 (11): 2128–40. [PubMed: 28436446]
- Lacagnina Michael J., Rivera Phillip D., and Bilbo Staci D.. 2017 "Glial and Neuroimmune Mechanisms as Critical Modulators of Drug Use and Abuse." *Neuropsychopharmacology: Official Publication of the American College of Neuropsychopharmacology* 42 (1): 156–77. [PubMed: 27402494]
- Lagace DC, Donovan MH, DeCarolis NA, Farnbauch LA, Malhotra S, Berton O, Nestler EJ, Krishnan V, Eisch AJ, 2010 Adult hippocampal neurogenesis is functionally important for stress-induced social avoidance. *Proc. Natl. Acad. Sci. U. S. A* 107, 4436–4441. [PubMed: 20176946]
- Liu Zhengyan, Fan Yang, Won Seok Joon, Neumann Melanie, Hu Dezhi, Zhou Liangfu, Weinstein Philip R., and Liu Jiaing. 2007 "Chronic Treatment with Minocycline Preserves Adult New Neurons and Reduces Functional Impairment after Focal Cerebral Ischemia." *Stroke; a Journal of Cerebral Circulation* 38 (1): 146–52.
- Lu Zhenjie, Elliott Michael R., Chen Yubo, Walsh James T., Klibanov Alexander L., Ravichandran Kodi S., and Kipnis Jonathan. 2011 "Phagocytic Activity of Neuronal Progenitors Regulates Adult Neurogenesis." *Nature Cell Biology* 13 (9): 1076–83. [PubMed: 21804544]
- Madisen Linda, Zwingman Theresa A., Sunkin Susan M., Seung Wook Oh Hatim A. Zariwala, Gu Hong, Ng Lydia L., et al. 2010 "A Robust and High-Throughput Cre Reporting and Characterization System for the Whole Mouse Brain." *Nature Neuroscience* 13 (1): 133–40. [PubMed: 20023653]
- Metz Verena E., Jones Jermaine D., Manubay Jeanne, Sullivan Maria A., Mogali Shanthi, Segoshi Andrew, Madera Gabriela, Johnson Kirk W., and Comer Sandra D.. 2017 "Effects of Ibudilast on the Subjective, Reinforcing, and Analgesic Effects of Oxycodone in Recently Detoxified Adults with Opioid Dependence." *Neuropsychopharmacology: Official Publication of the American College of Neuropsychopharmacology* 42 (9): 1825–32. [PubMed: 28393896]
- Michaud Jean-Philippe, Richard Karine L., and Rivest Serge. 2012 "Hematopoietic MyD88 Adaptor Protein Acts as a Natural Defense Mechanism for Cognitive Deficits in Alzheimer's Disease." *Stem Cell Reviews and Reports* 8 (3). Humana Press Inc: 898–904. [PubMed: 22374079]
- Noonan Michele A., Bulin Sarah E., Fuller Dwain C., and Eisch Amelia J.. 2010 "Reduction of Adult Hippocampal Neurogenesis Confers Vulnerability in an Animal Model of Cocaine Addiction." *The Journal of Neuroscience: The Official Journal of the Society for Neuroscience* 30 (1): 304–15. [PubMed: 20053911]
- Northcutt AL, Hutchinson MR, Wang X, Baratta MV, Hiranita T, Cochran TA, Pomrenze MB, et al. 2015 "DAT Isn't All That: Cocaine Reward and Reinforcement Require Toll-like Receptor 4 Signaling." *Molecular Psychiatry* 20 (12): 1525–37. [PubMed: 25644383]
- Okun Eitan, Barak Boaz, Saada-Madar Ravit, Rothman Sarah M., Griffioen Kathleen J., Roberts Nicholas, Castro Kamilah, et al. 2012 "Evidence for a Developmental Role for TLR4 in Learning and Memory." *PloS One* 7 (10): e47522. [PubMed: 23071817]
- Onaivi Emmanuel S., Ishiguro Hiroki, Gong Jian-Ping, Patel Sejal, Meozzi Paul A., Myers Lester, Perchuk Alex, et al. 2008 "Brain Neuronal CB2 Cannabinoid Receptors in Drug Abuse and Depression: From Mice to Human Subjects." *PloS One* 3 (2): e1640. [PubMed: 18286196]
- Parkhurst Christopher N., Yang Guang, Ninan Ipe, Savas Jeffrey N., Yates John R., 3rd, Lafaille Juan J., Hempstead Barbara L., Littman Dan R., and Gan Wen-Biao. 2013 "Microglia Promote

- Learning-Dependent Synapse Formation through Brain-Derived Neurotrophic Factor.” *Cell* 155 (7): 1596–1609. [PubMed: 24360280]
- Ray Lara A., Bujarski Spencer, Shoptaw Steve, Roche Daniel Jo, Heinzerling Keith, and Miotto Karen. 2017 “Development of the Neuroimmune Modulator Ibudilast for the Treatment of Alcoholism: A Randomized, Placebo-Controlled, Human Laboratory Trial.” *Neuropsychopharmacology: Official Publication of the American College of Neuropsychopharmacology* 42 (9): 1776–88. [PubMed: 28091532]
- Reshef Ronen, Kreisel Tirzah, Kay Dorsa Beroukhim, and Yirmiya Raz. 2014 “Microglia and Their CX3CR1 Signaling Are Involved in Hippocampal- but Not Olfactory Bulb-Related Memory and Neurogenesis.” *Brain, Behavior, and Immunity* 41 (October): 239–50.
- Rivera Phillip D., Raghavan Ramya K., Yun Sanghee, Latchney Sarah E, McGovern M-K, García Emily F., Birnbaum Shari G., and Eisch Amelia J. 2015 “Retrieval of morphine-associated context induces cFos in dentate gyrus neurons.” *Hippocampus* 25: 409–414. [PubMed: 25424867]
- Rogers Justin T., Morganti Josh M., Bachstetter Adam D., Hudson Charles E., Peters Melinda M., Grimmig Bethany A., Weeber Edwin J., Bickford Paula C., and Gemma Carmelina. 2011 “CX3CR1 Deficiency Leads to Impairment of Hippocampal Cognitive Function and Synaptic Plasticity.” *The Journal of Neuroscience: The Official Journal of the Society for Neuroscience* 31 (45). *Soc Neuroscience*: 16241–50. [PubMed: 22072675]
- Rolls Asya, Shechter Ravid, London Anat, Ziv Yaniv, Ronen Ayal, Levy Rinat, and Schwartz Michal. 2007 “Toll-like Receptors Modulate Adult Hippocampal Neurogenesis.” *Nature Cell Biology* 9 (9): 1081–88. [PubMed: 17704767]
- Schwarz Jaclyn M., Hutchinson Mark R., and Bilbo Staci D.. 2011 “Early-Life Experience Decreases Drug-Induced Reinstatement of Morphine CPP in Adulthood via Microglial-Specific Epigenetic Programming of Anti-Inflammatory IL-10 Expression.” *The Journal of Neuroscience: The Official Journal of the Society for Neuroscience* 31 (49): 17835–47. [PubMed: 22159099]
- Sekine Yoshimoto, Ouchi Yasuomi, Sugihara Genichi, Takei Nori, Yoshikawa Etsuji, Nakamura Kazuhiko, Iwata Yasuhide, et al. 2008 “Methamphetamine Causes Microglial Activation in the Brains of Human Abusers.” *The Journal of Neuroscience: The Official Journal of the Society for Neuroscience* 28 (22): 5756–61. [PubMed: 18509037]
- Shen Kimberle, Sidik Harwin, and Talbot William S.. 2016 “The Rag-Ragulator Complex Regulates Lysosome Function and Phagocytic Flux in Microglia.” *Cell Reports* 14 (3): 547–59. [PubMed: 26774477]
- Sierra Amanda, Beccari Sol, Irune Diaz-Aparicio Juan M. Encinas, Comeau Samuel, and Tremblay Marie-Ève. 2014 “Surveillance, Phagocytosis, and Inflammation: How Never-Resting Microglia Influence Adult Hippocampal Neurogenesis.” *Neural Plasticity* 2014 (March): 610343. [PubMed: 24772353]
- Sierra Amanda, Encinas Juan M., Deudero Juan J. P., Chancey Jessica H., Enikolopov Grigori, Overstreet-Wadiche Linda S., Tsirka Stella E., and Maletic-Savatic Mirjana. 2010 “Microglia Shape Adult Hippocampal Neurogenesis through Apoptosis-Coupled Phagocytosis.” *Cell Stem Cell* 7 (4): 483–95. [PubMed: 20887954]
- Sriram Krishnan, and O’Callaghan James P.. 2007 “Divergent Roles for Tumor Necrosis Factor- α in the Brain.” *Journal of Neuroimmune Pharmacology* 2 (2). Kluwer Academic Publishers-Plenum Publishers: 140–53. [PubMed: 18040839]
- Stevens CW, Aravind S, Das S, and Davis RL. 2013 “Pharmacological Characterization of LPS and Opioid Interactions at the Toll-like Receptor 4.” *British Journal of Pharmacology* 168 (6): 1421–29. [PubMed: 23083095]
- Theberge Florence R., Li Xuan, Kambhampati Sarita, Pickens Charles L., St Laurent Robyn, Bossert Jennifer M., Baumann Michael H., et al. 2013 “Effect of Chronic Delivery of the Toll-like Receptor 4 Antagonist (+)-Naltrexone on Incubation of Heroin Craving.” *Biological Psychiatry* 73 (8): 729–37. [PubMed: 23384483]
- Tzschentke Thomas M. 2007 “Measuring Reward with the Conditioned Place Preference (CPP) Paradigm: Update of the Last Decade.” *Addiction Biology* 12 (3–4): 227–462. [PubMed: 17678505]
- Wang Xiaohui, Loram Lisa C., Ramos Khara, de Jesus Armando J., Thomas Jacob, Cheng Kui, Reddy Anireddy, et al. 2012 “Morphine Activates Neuroinflammation in a Manner Parallel to

- Endotoxin." Proceedings of the National Academy of Sciences of the United States of America 109 (16): 6325–30. [PubMed: 22474354]
- Williamson Lauren L., Sholar Paige W., Mistry Rishi S., Smith Susan H., and Bilbo Staci D.. 2011 "Microglia and Memory: Modulation by Early-Life Infection." The Journal of Neuroscience: The Official Journal of the Society for Neuroscience 31(43): 15511–21 [PubMed: 22031897]
- Yirmiya Raz, and Goshen Inbal. 2011 "Immune Modulation of Learning, Memory, Neural Plasticity and Neurogenesis." Brain, Behavior, and Immunity 25 (2): 181–213.
- Yona Simon, Kim Ki-Wook, Wolf Yochai, Mildner Alexander, Varol Diana, Breker Michal, Strauss-Ayali Dalit, et al. 2013 "Fate Mapping Reveals Origins and Dynamics of Monocytes and Tissue Macrophages under Homeostasis." Immunity 38 (1): 79–91. [PubMed: 23273845]
- Zabel Matthew K., Zhao Lian, Zhang Yikui, Gonzalez Shaimar R., Ma Wenxin, Wang Xu, Fariss Robert N., and Wong Wai T.. 2016 "Microglial Phagocytosis and Activation Underlying Photoreceptor Degeneration Is Regulated by CX3CL1-CX3CR1 Signaling in a Mouse Model of Retinitis Pigmentosa." Glia 64 (9): 1479–91. [PubMed: 27314452]
- Zhang Ye, Chen Kenian, Sloan Steven A., Bennett Mariko L., Scholze Anja R., O’Keeffe Sean, Phatnani Hemali P., et al. 2014 "An RNA-Sequencing Transcriptome and Splicing Database of Glia, Neurons, and Vascular Cells of the Cerebral Cortex." The Journal of Neuroscience: The Official Journal of the Society for Neuroscience 34 (36). Society for Neuroscience: 11929–47. [PubMed: 25186741]
- Zhang Yue, Xu Chi, Zheng Hui, Loh Horace H., and Law Ping-Yee. 2016 "Morphine Modulates Adult Neurogenesis and Contextual Memory by Impeding the Maturation of Neural Progenitors." PloS One 11 (4): e0153628. [PubMed: 27078155]

- Addiction-like behaviors are enhanced in mice with microglial MyD88 deletion
- Morphine leads to aberrant levels of immature neurons in the dentate gyrus
- Morphine leads to dysfunction of microglial lysosomes containing immature neurons
- Microglial MyD88 signaling may be protective regarding addiction-like behaviors

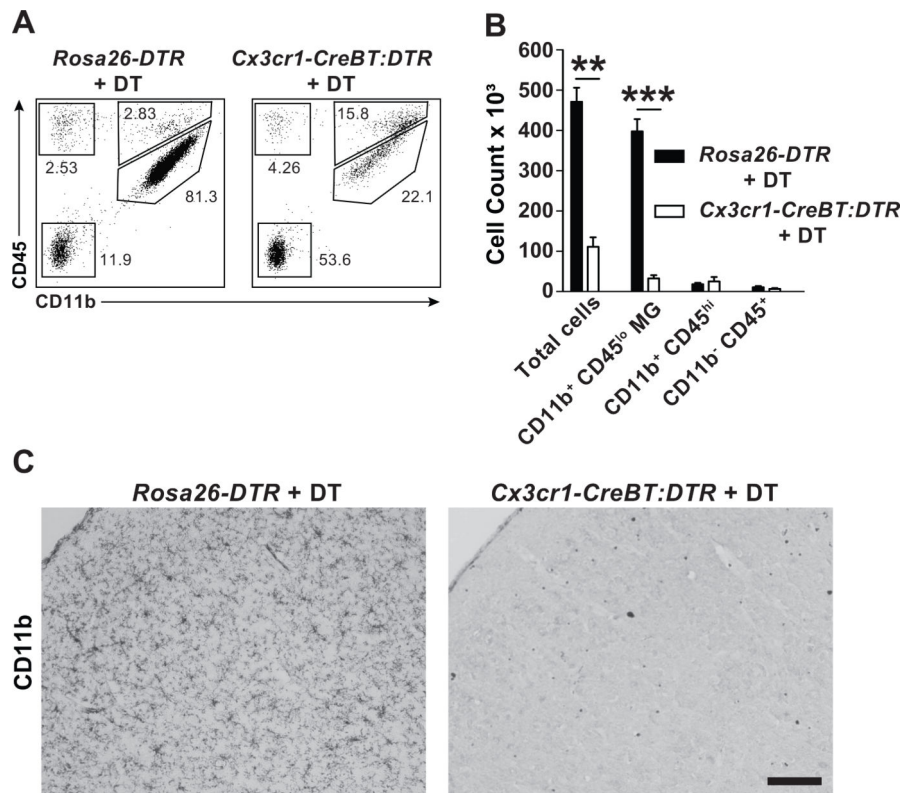


Figure 1. Selective depletion of parenchymal microglia in *Cx3cr1-CreBT:DTR* mice. (A) Total brain leukocytes as determined by flow cytometry in *Rosa26-DTR* and *Cx3cr1-CreBT:DTR* mice 24 hrs after treatment with 50 ng/kg DT (i.p. daily for 3 days). Plots are gated on total live CD45⁺ cells and subgated into microglia (CD11b⁺ CD45^{low}), myeloid (CD11b⁺ CD45^{high}), lymphoid (CD11b⁻ CD45^{high}), and non-immune (CD45⁻) cells. (B) Quantification of absolute number of cells after treatment as described in A. **p<0.01, ***p<0.001 by Student's *t* test. (C) CD11b immunohistochemical staining in the frontal cortex of *Rosa26-DTR* and *Cx3cr1-CreBT:DTR* mice after DT treatment as described in A. Mean±SEM. Scale bar: 100 μm.

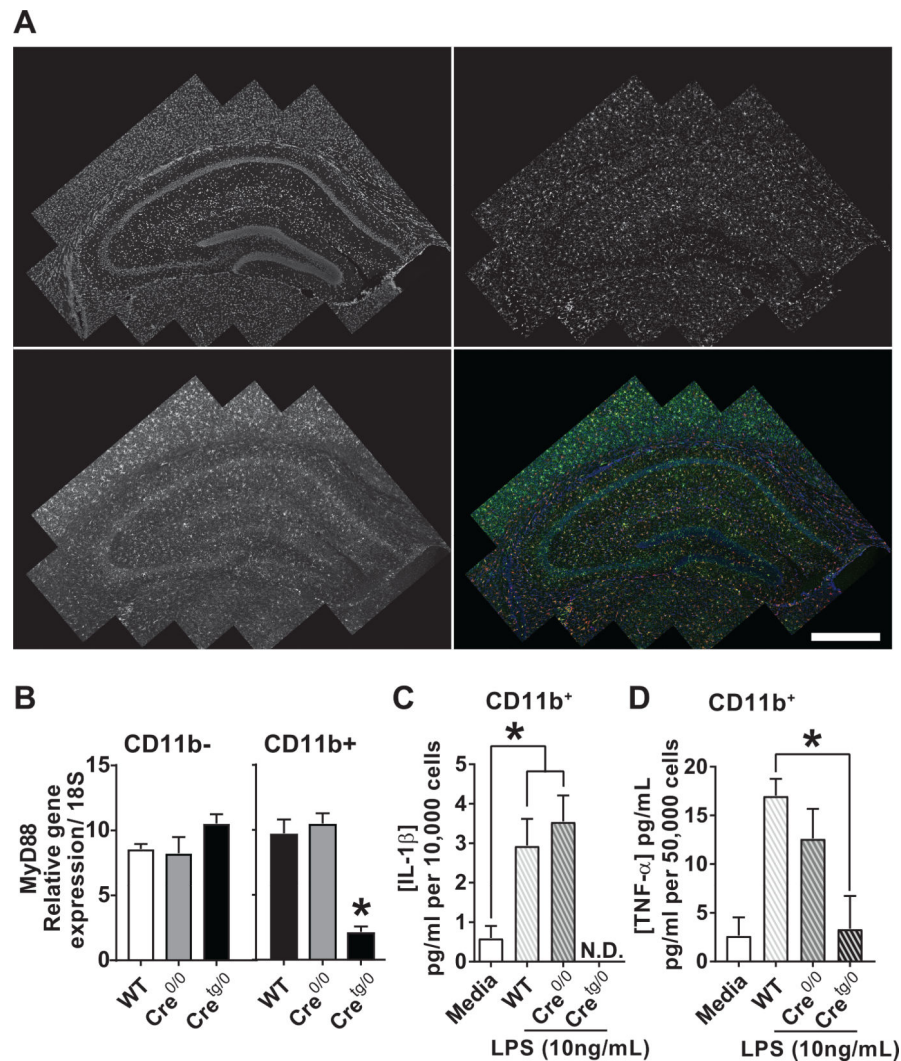


Figure 2. Within the CNS, *Cx3cr1-CreBT* mice label and disrupt parenchymal microglia. (A) Hippocampus of a 4 week-old *Cx3cr1-CreBT:tdTomato^{fl/wt}* mouse showing tdTomato, Iba-1, DAPI, and merged markers. (B) Microglial isolations of samples from WT, Cre^{0/0}, and Cre^{tg/0} separated by CD11b⁻ and CD11b⁺ populations (n=3/group). The relative gene expression levels of *MyD88* was normalized to *18S*. Student's *t*-test, *P<0.05. (C,D) ELISA protein concentrations for IL-1β (C, n=3) and TNFα (D, n=3) were normalized to 10,000 or 50,000 cells, respectively. *P<0.05 by One-way ANOVA. N.D., not detectable. Mean±SEM. Scale bar, 1mm.

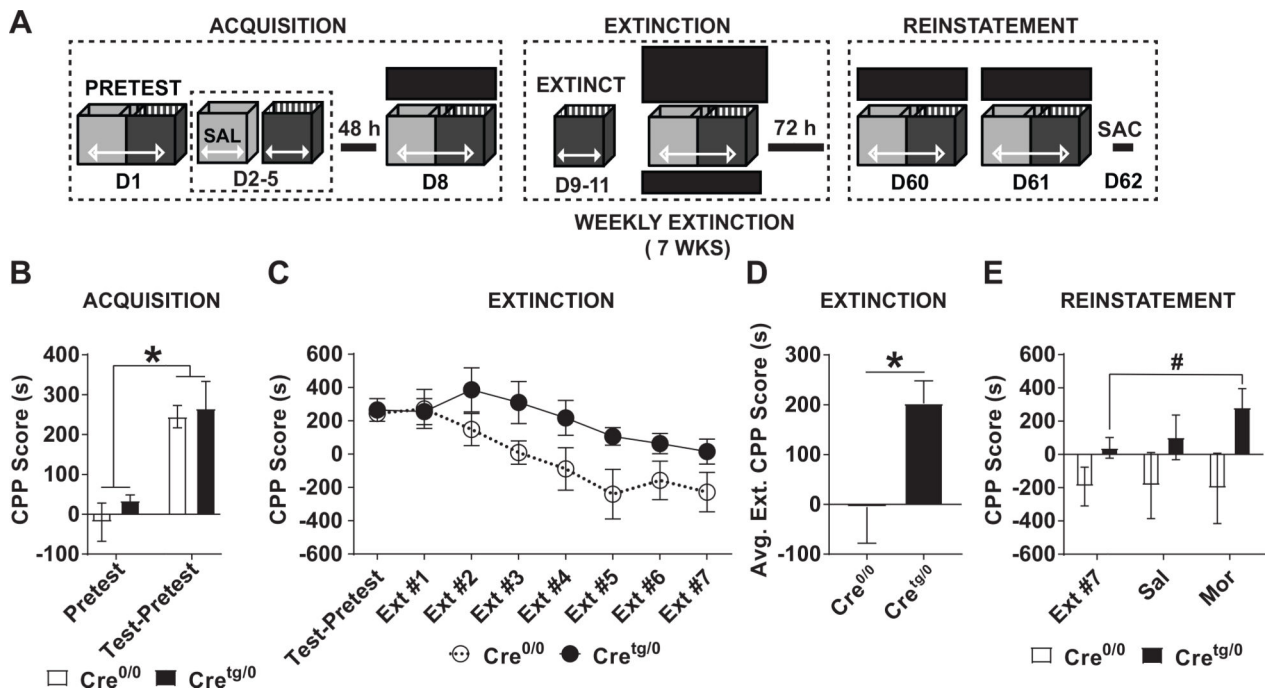


Figure 3. Addition-like behaviors assessed by low dose morphine CPP are enhanced in Cre^{tg/0}, compared to Cre^{0/0} mice.

(A) Schematic of morphine CPP (3 mg/kg) acquisition, extinction, and reinstatement experiment. (B) Acquisition was examined on D8 of the mCPP paradigm. (C-D) Extinction testing of mCPP was performed weekly for 7 weeks. (C) Weekly and (D) averaged extinction tests are shown. *P<0.05, Student *t*-test. (E) Reinstatement to saline (D60) and morphine (D61, 3 mg/kg, s.c.) was performed. **P<0.01, *P<0.05 two-way ANOVA, Mean ±SEM. SAL, saline; MOR, morphine.

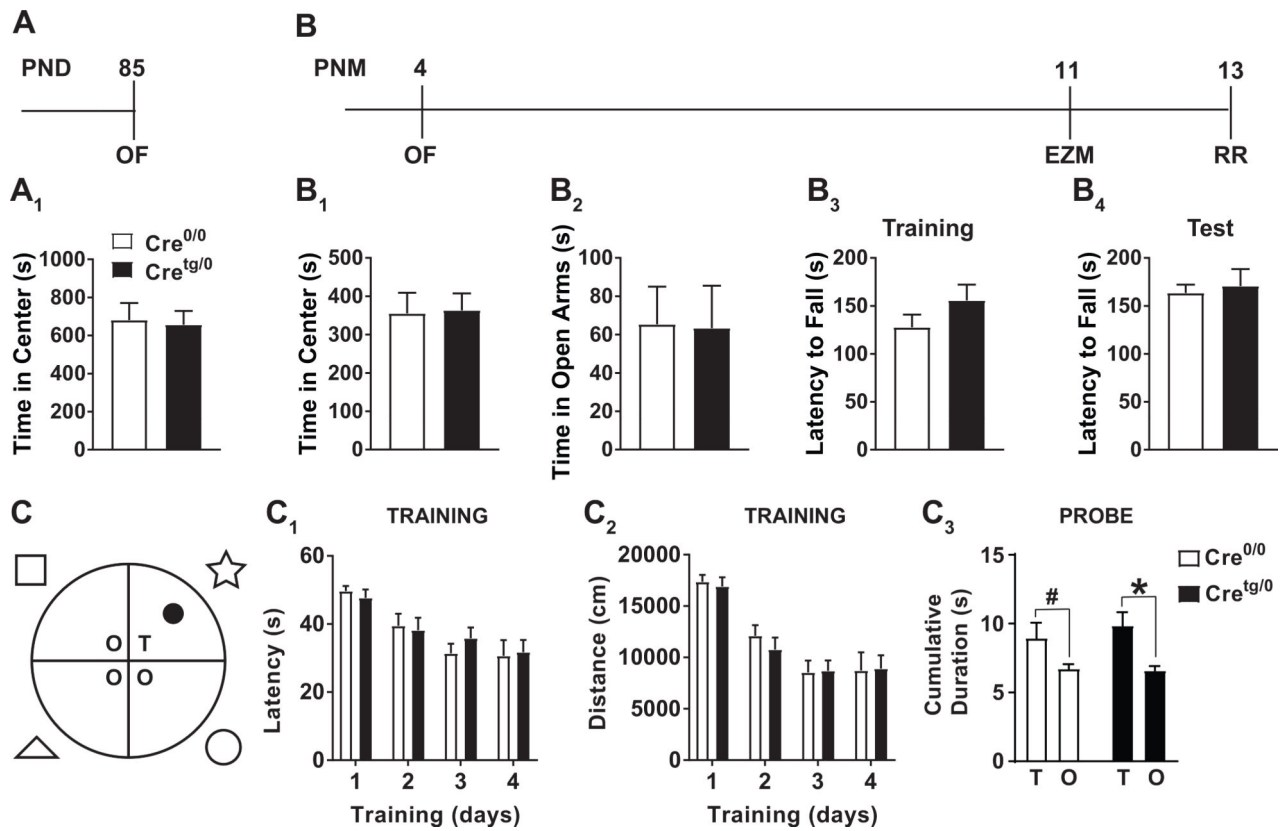


Figure 4. Anxiety-like, motor, and learning and memory behaviors are not different between Cre^{0/0} and Cre^{tg/0} mice.

(A-B) Timeline of behaviors performed on (A) PND 85 and (B) postnatal month (PNM) 4 Cre^{tg/0} and Cre^{0/0} mice. (A1) OF behavior was performed on PND 85 mice. (B1-B4) In a separate group of mice, starting at PNM 4, open field (OF), elevated zero maze (EZM), and rota-rod (RR) was performed. (C) Diagram of MWM with spatial cues used for spatial learning and memory. (C1,2) Training days 1–4 for Cre^{tg/0} and Cre^{0/0} mice examining latency to find the hidden platform (C1) and total distance travelled before finding the hidden platform (C2). (C3) Probe tests examining the cumulative duration in target quadrant (T) compared to other quadrants (O) showed a main effect of Quadrant ($F(1,24)=7.736$, $P<0.05$), but no Genotype ($F(1,24)=0.5375$) or significant interaction ($F(1,24)=0.2666$) by repeated measures two-way ANOVA. Post-hoc analysis * $p<0.05$, # $p<0.05$ Student's *t*-test. Mean±SEM.

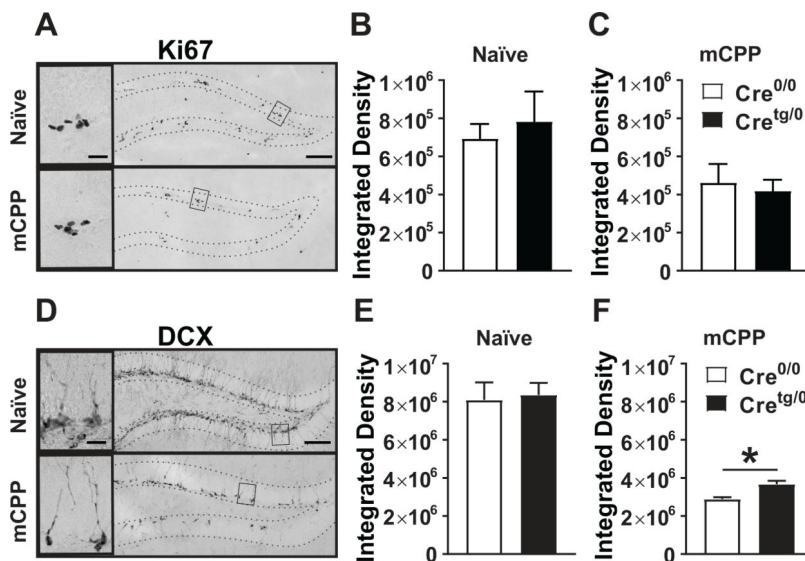


Figure 5. Doublecortin, but not Ki67, levels are increased in Cre^{tg/0} mice only after mCPP. (A,D) Images of Ki67 (A) and DCX (D) DG were obtained by drawing ROIs of the SGZ or GCL, respectively, and performing maximum projections of z-stacks. Top, Naïve; Bottom, mCPP. Thresholding was applied using ImageJ and the integrated density of the Ki67 or DCX signal within the ROI was obtained. (B,C,E,F) The integrated density of Ki67 (B,C) and DCX (E,F) within the DG of PND 120 mice that are (B,E) naïve and (C,F) mCPP mice are shown. *P<0.05, Student *t*-test. Mean±SEM. Scale bars, 100um, insets 20um.

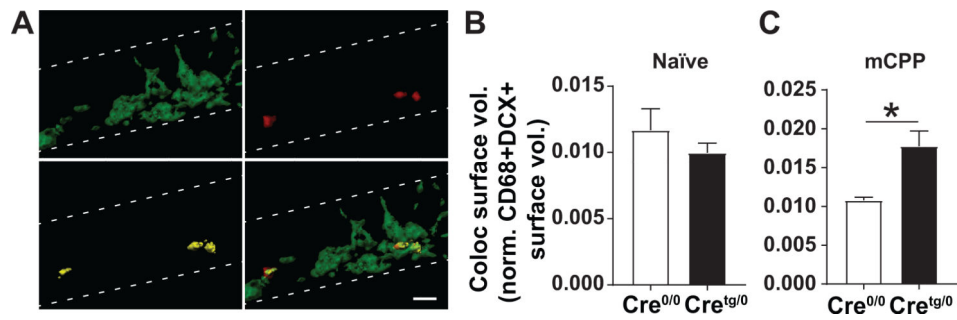


Figure 6. The lysosomal volumes of microglia that contain immature neuronal debris from Cre^{tg/0} mice are increased, compared to Cre^{0/0} controls.

(A) The 3D-rendered surface volumes for DCX, CD68, Colocalization, and merged channels in the DG are shown. (B-C) Colocalized surface volumes normalized to the DCX+ and CD68+ signal within the DG for (B) naïve and (C) mCPP groups. Coloc., colocalization; Vol., volume.; Norm., normalized. *P<0.05, Student *t*-test. Mean±SEM. Scale bar, 10um.

Author Manuscript

Author Manuscript

Author Manuscript

Author Manuscript

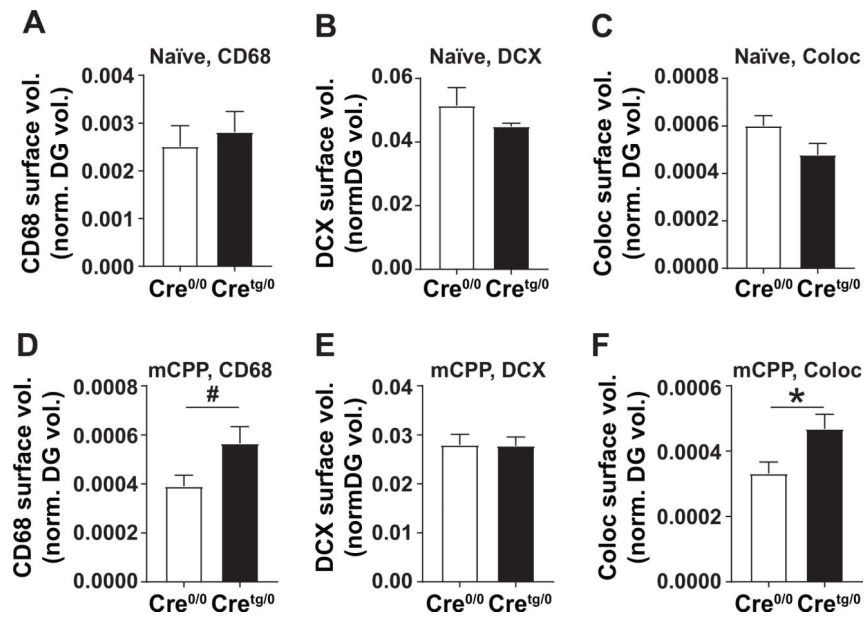


Figure 7. Surface volumes of CD68+, DCX+, and Colocalized DCX+CD68+ signal within the DG vary depending on mCPP testing.

(A-F) The 3D-rendered surface volumes for (A, D) CD68, (B, E) DCX, and (C, F) colocalization were measured and normalized to the total DG volume in (A-C) naïve and (D-F) mCPP groups. Coloc, colocolaization. #p=0.06, *p<0.05 by Student’s *t*-test. Mean±SEM.

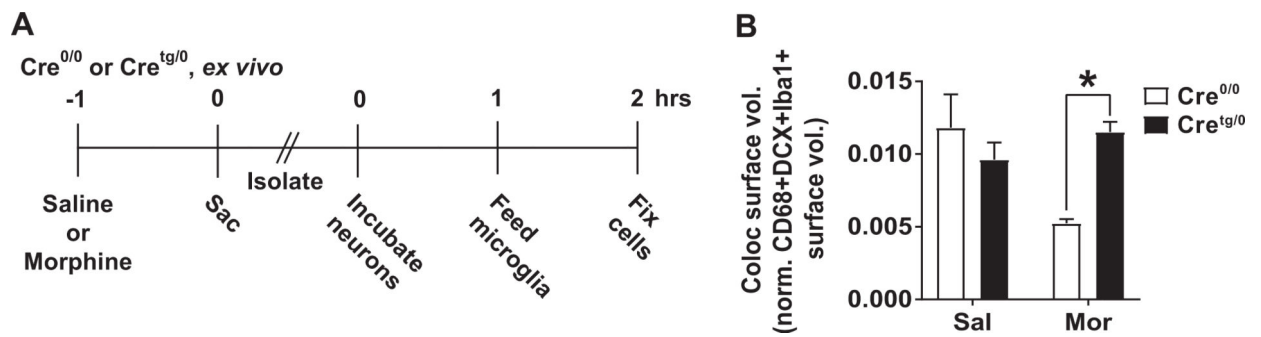


Figure 8. Surface volumes of colocalized DCX+CD68+Iba1+ signal vary depending on treatment and genotype.

(A) Timeline of *ex vivo* experiment performed on Cre^{tg/0} and Cre^{0/0} mice. (B) The 3D-rendered surface volume for DCX+CD68+Iba1+ colocalization was determined after saline or morphine treatment of Cre^{tg/0} and Cre^{0/0} mice. A significant interaction (F(1,7)=7.797) by two-way ANOVA was found and no main effects of genotype (F(1,7)=1.799) or treatment (F(1,7)=2.37) were observed. Student's *t*-test *p<0.05. Mean±SEM.